

STUDY OF MACRO- AND MICRO-STRUCTURE AND MORPHOLOGICAL EVALUATION OF GRAPHITE IN A NODULAR CAST IRON OBTAINED BY CASTING IN THE FORM OF AN INGOT

Lucas dos Santos Souza

Advanced Materials Laboratory, Science and
Technology Center – UENF – Campos dos
Goytacazes, Brazil

Lioudmila Aleksandrovna Matlakhova

Advanced Materials Laboratory, Science and
Technology Center – UENF – Campos dos
Goytacazes, Brazil

Natalia Alekseevna Palii

Baykov Metallurgy and Materials Institute –
IMET – Moscow, Russia

Sérgio Neves Monteiro

Military Institute of Engineering – IME – Rio
de Janeiro, Brazil

All content in this magazine is
licensed under a Creative Com-
mons Attribution License. Attri-
bution-Non-Commercial-Non-
Derivatives 4.0 International (CC
BY-NC-ND 4.0).



Abstract: Cast irons are Fe-C-Si alloys with carbon content above 2%, and nodular or ductile cast iron is characterized by having free carbon in the form of spheroidal graphite nodules. The objective of the current work is the systematic study of the macro- and micro-structure of a nodular cast iron, obtained by casting in the form of an ingot in a sand mold, correlating the structural and morphological aspects of the graphite nodules with solidification. The material studied was provided by the company Pam Saint-Gobain Canalização, located in Barra Mansa-RJ, Brazil. For the analysis, the central part of the ingot was selected and a 1 cm thick profile was removed through a total cross-section. The entire profile was metallographically prepared. Structural analysis was performed by optical microscopy, applying qualitative and quantitative evaluation techniques. As a result, it was determined that the size and quantity of nodules per area vary within the same ingot, according to the solidification profile. Regions closer to the surface of the ingot, where the cooling speed is higher, the average size of the graphite nodules was smaller and with a higher concentration per area, than in the central regions, where cooling is slower and the size of the nodules was larger and smaller number of nodules per area. Also, in the central region of the ingot, macrodefects in the form of pores and voids were observed. It is concluded that the variation in the speed at which cooling occurs, resulting from heat extraction rates and thermal gradients at each moment of solidification, is a determining factor for the alteration of the microstructure of the nodular cast iron ingot.

Keywords: Nodular Cast Iron; Macroanalysis and microanalysis of the ingot; Microstructure and Mechanical Properties; Distribution and size of graphite nodules.

INTRODUCTION

Cast irons, since the beginning, have always been considered materials of great importance and interest to ancient civilizations, however, they had limited use due to their fragility. Advances in the fields of research and technology, provided the development of new and diversified methods of obtaining, as well as changing its structure and properties, resulting in different types of cast iron. Among these, nodular cast iron (FFN) stands out for its excellent combination of high ductility combined with good mechanical strength, making this alloy replace other cast irons, as well as some types of steel, as it has a lower production cost. These qualities are responsible for the application of FFNs in various segments, such as the production of parts for the automobile industry, the production of pipes and connections for the transport of water, valves and pump bodies in the oil industry. According to the literature, world production of ductile cast iron is constantly growing and it is estimated that annual production exceeds 25 million tons (Vidal, 2013; Lacaze et al, 2021).

FFNs are Fe-C-Si alloys, with C content above 2.0%, in which the free carbon is found in the form of spheroidal graphite nodules present in the metallic matrix, which can be ferrite, pearlite, bainite and/or austenite. Nodular graphite allows the continuity of the matrix, which allows plastic deformation without fragility, as in the case of graphite lamellae in gray cast iron. In ferritic matrix FFNs, the resistance limit varies from 380 to 450 MPa, associated with an elongation of 7 to 22%, while in pearlitic matrix FFNs, the resistance limit can reach 900 MPa, with elongation of up to 2% (Guesser, 2019; Chiaverini, 2012).

The FFNs are obtained by inoculation and nodulation treatments, carried out with the metal still in the liquid state. Inoculation

consists of adding a graphitizing element, usually silicon (Si), in order to favor the formation of free carbon, in the form of graphite. However, in the presence of active surface elements, such as sulfur (S) and oxygen (O), graphite has a lower interface energy in its prismatic plane, which results in lamellar graphite, characteristic of gray cast iron, more brittle and less ductile (Santos and Branco, 1989; Fras and Gorny, 2012). In nodulation, magnesium (Mg) is added, which reacts with S, O and other impurity elements, removing them from the metallic bath and forming oxides and sulfides, while volatilizing. With the removal of S and O, the graphite basal planes will have lower interface energy with the metallic bath. This way, the graphite will grow perpendicular to the basal plane, resulting in the formation of graphite nodules (Stefanescu, 2005).

Casting process, solidification and formation of crystalline structure starts from the walls of the mold, proceeding towards the center of the ingot. During the solidification of a FFN, several processes can occur, accompanying the heat extraction, including: thermal gradients at each moment of solidification; cooling with variable speeds per region of the ingot; liquid-solid phase transformations, eutectic and eutectoid reactions; change in the solubility of carbon and other alloying elements in austenite; and precipitation of free or bound carbon (Santos and Branco, 1989).

The objective of this work is the systematic study of the macro and microstructure of a nodular cast iron, obtained by casting in the form of an ingot, correlating structural and morphological aspects of the graphite nodules with the solidification of the ingot.

MATERIALS AND METHODOLOGY

MATERIALS

The FFN ingot analyzed was produced by the company Pam Saint-Gobain Canalização, located in Barra Mansa-RJ, Brazil. In production, Fe-Si (75% Si) was added to the pig iron metallic bath for the inoculation treatment, and Mg for the nodulization treatment, using the bell immersion technique (Vidal, 2013). The CP Ybloc ingot was obtained from a mass of liquid metal (4470 Kg) with an initial temperature of 1502°C, which was treated with 8.8 Kg of Mg for nodulation and with 24 Kg of Fe-Si75% for inoculation, being poured into a sand mold, 15 min after the end of the treatments at a temperature of 1326 °C (called T15). The chemical compositions of FFN before and after treatments are shown in Table 1.

The ingot was sectioned, according to the scheme shown in Figure 1. A large sample, corresponding to the profile of the ingot, for macro and microstructural analysis, was taken by two total transverse cuts in the central part of the ingot, having a thickness of about 10 mm (Figure 1-a).

METHODS

METALLOGRAPHIC TESTS

The sample from the cross section, corresponding to the profile of the ingot (T15), was made following metallographic preparation techniques, which included: cutting, cold embedding with acrylic resin, sanding and polishing. Finally, images of its macro and microstructure were obtained, in order to observe the morphological aspect of the graphite nodules and constituents.

For the characterization of sample T15, two observation techniques were used. A macrostructural one, to determine the characteristics of the ingot, influenced

by the casting process, through visual observation and with the aid of a magnifying glass. The other, microstructural, with the purpose of evaluating the size, distribution and morphology of the graphite nodules according to the regions of the ingot, using the Neophot-32 optical microscope.

The microstructural analysis of sample T15 was carried out systematically, similar to that of a Cartesian plane (Figure 1-c), where every 5.0 mm vertically and horizontally an image of its microstructure was obtained, with two magnifications, 50 and 100x magnification and two observation methods, brightfield and darkfield. Thus, having the origin (0,0), or point of zero line and zero column at the upper left end of the sample, as it moved to the right and down, values were added, corresponding to the distance from the point of origin, in the coordinates, columns and rows, respectively. This way, it was possible, through a coordinate, to identify which region the obtained micrograph corresponded to in the profile sample of the ingot.

Quantitative analysis of the micrographs followed two methods. The first consisted of creating previously calibrated circles on the nodules and measuring their sizes, obtaining histograms of the amount of graphite nodules by established size ranges, the graphite volumetric fraction and the average size of the nodules. This method proved to be very efficient in quantitatively evaluating the microstructure of FFNs (Vidal, 2017). However, its realization demanded a lot of time, which made it time-consuming and tiring to be executed for the analysis of many images. The second method included the use of the *Image J program*, adapted for this research. This method proved to be faster and less tiring to execute. It presented results compatible with the method of overlapping circles. However, as it is a computerized technique, it was necessary to make manual

adjustments during the evaluation with the program, so that it correctly recognized the graphite nodules.

RESULTS AND DISCUSSION

MACROSTRUCTURAL ANALYSIS

The analysis of the T15 sample, taken from the center of the ingot and metallographically prepared until polishing, revealed the presence of pores and voids in the central region of the ingot, with good homogeneity in the other regions (Figure 1-b). Pores and voids in the ingot can be explained as coming from the casting process, due to the emission and retention of gases during solidification. The change in material density during cooling causes the emitted gases to migrate to the center of the ingot, where they are trapped (Chiaverini, 2012; Baldam and Vieira, 2013).

QUALITATIVE MICROSTRUCTURAL ANALYSIS OF SAMPLE T15

The micrographs in Figures 2 and 3 (ah) illustrate the variations in the morphology of the graphite nodules of sample T15 along two vertical lines, corresponding to columns 10 and 20, highlighted in Figure 1-c.

By observing the micrographs of the polished T15 sample (Figures 2 and 3), it is possible to notice the presence of graphite in the form of nodules, characteristic of FFNs according to ISO 945-1/2019. In addition, it must be noted that in regions close to the upper end of the sample, as in images a) and b) of Figures 2 and 3, the graphite nodules are smaller and in greater quantity per area than in the central regions of the ingot, as in images e) and f) of the same figures, which have larger and smaller nodules per area. Likewise, when observing regions close to the lower end of the sample, images g) and h) of Figures 2 and 3, the graphite nodules were smaller and in greater quantity per area.

Figure 4 illustrates the microstructure

ELEMENT (%p)	Ç	yes	Mn	P	s	mg
before treatments	3.86%	2.18%	0.21%	0.08%	0.015%	-
after the treatments	3.61%	2.44%	0.2%	0.083%	0.009%	0.092%

Table 1: Chemical composition of the FFN T15 ingot before and after the inoculation and nodulation treatments.

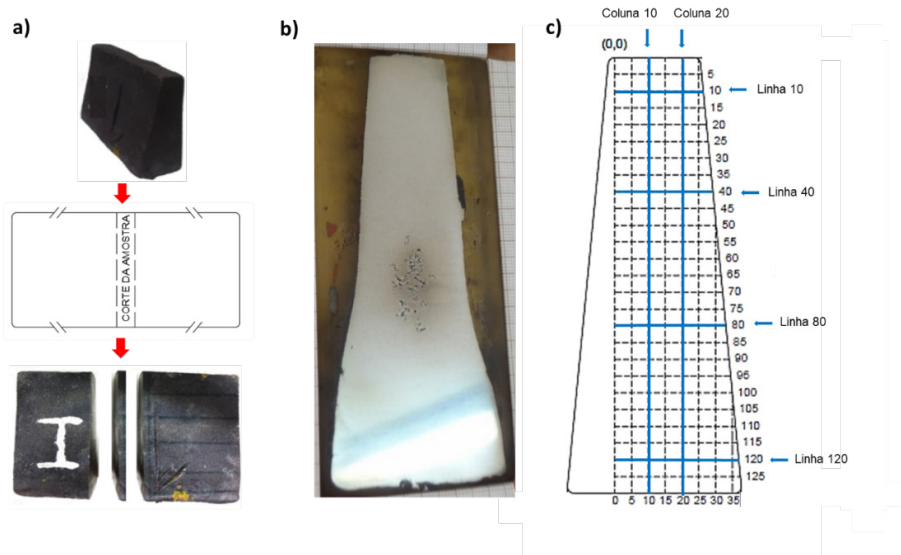


Figure 1: Ingot CP Ybloc: a) Scheme of cutting the central part of the ingot to obtain the sample, b) large cross-sectional sample, sanded and polished, and c) schematic of the sample's metallographic analysis.

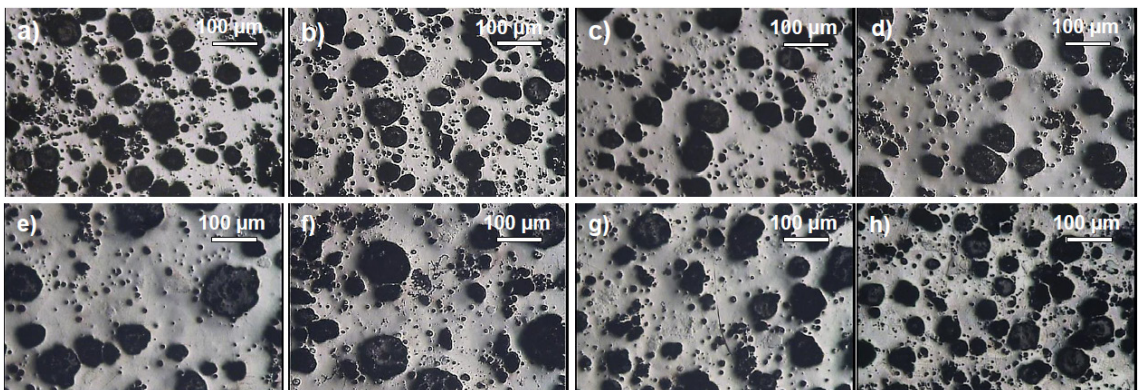


Figure 2: Microstructure of the T15 FFN sample in several regions, coordinates in mm: a) (10.5); b) (10,10); c) (10.20); d) (10.30); e) (10.40); f) (10.55); g) (10.80); h) (10.120) Polished state; Magnification 100x; Observation regime: bright field.

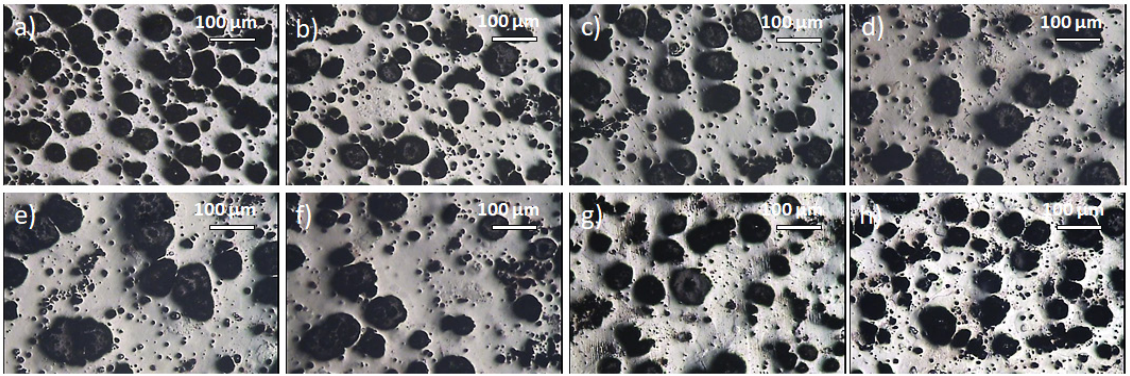


Figure 3: Microstructure of the FFN T15 sample in several regions, coordinates in mm: a) (20.5); b) (20.10); c) (20,20); d) (20.45); e) (20.60); f) (20.85); g) (20.100); h) (20,120) Polished state; Magnification 100x; Observation regime: bright field.

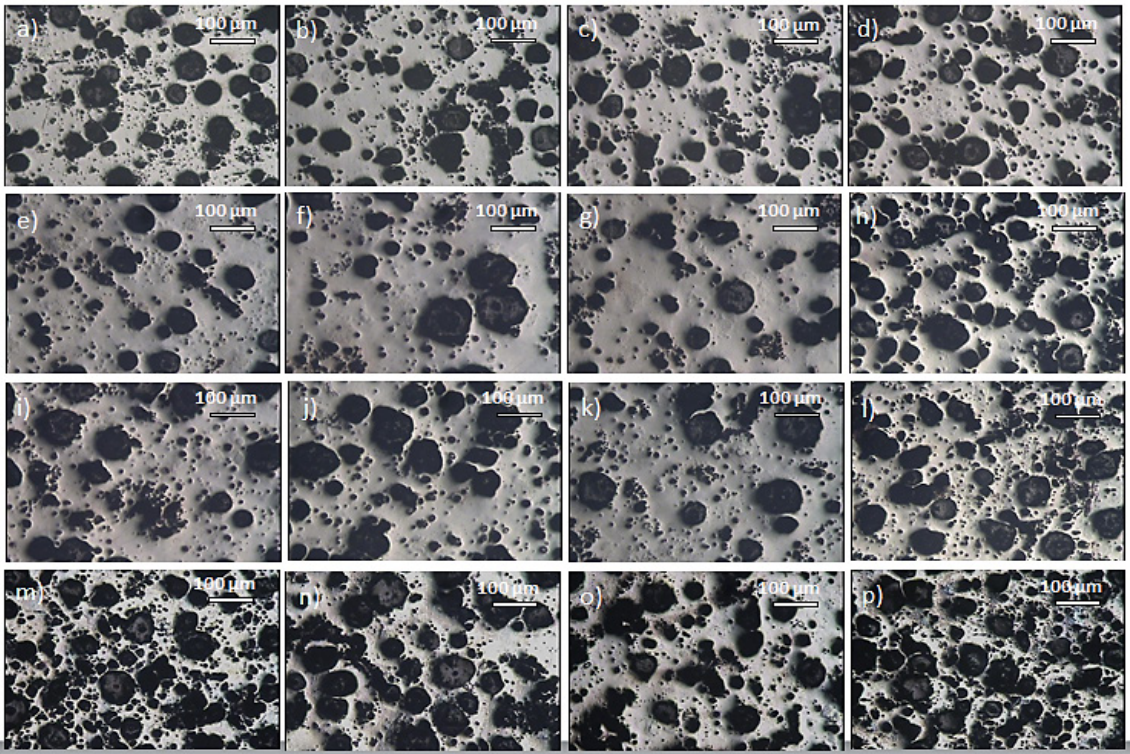


Figure 4: Microstructure of the T15 FFN sample in several regions, coordinates in mm: a) (0.10); b) (5.10); c) (15.10); d) (20.10); e) (0.40); f) (5.40); g) (15.40); h) (27.40); i) (0.80); j) (15.80); k) (25.80); l) (33.80); m) (0.120); n) (15.120); o) (25,120); p) (35.120)

Polished state; Magnification 100x; Observation regime: bright field.

variation of sample T15, according to four horizontal lines of analysis, corresponding to lines 10, 40, 80 and 120, highlighted in Figure 1 -c. This way, it can be observed that the lateral extremities, images d), h), l) and p), also present the effect of reducing the size and increasing the number of graphite nodules. Thus, the closer to the edge or surface of the ingot, the greater the number of nodules per area and the smaller their size.

QUANTITATIVE MICROSTRUCTURAL ANALYSIS OF SAMPLE T15 COMPARISON BETWEEN THE EVALUATION BY THE OVERLAPPING CIRCLE METHODS AND BY THE IMAGE J PROGRAM

The variation in the sizes of the graphite nodules, observed during the qualitative analysis, was quantified through the techniques of overlapping circles, Figure 5 (a), and through the *Image J program*, Figure 5 (b).

Table 2 presents the values of the mean size (μm), number of nodules per mm^2 and volumetric fraction (%), identified by the two methods.

Figure 6 shows the comparison of the results obtained by the method of overlapping circles and the *Image J program* for evaluating the number of nodules per mm^2 in certain ranges of sizes.

By comparing the images in Figure 5 (a, b) it can be seen that the *Image J program* is more efficient in delimiting the perimeter (or contour) of the nodules, since the description of the graphite nodule by a circle, as in the method of overlapping circles, consists of an approximation. From the histogram in Figure 6, it can be seen that the *Image J program* has comparable results to the circle overlapping method. Furthermore, it is more efficient in measuring very small nodules (0-10 μm),

which are more difficult to quantify. Table 2 presents the main results of the evaluations by each method, where the differences between the results expressed by the two methods can be associated with the fact that the *Image J program* is more efficient in delimiting the size of the nodules, as well as in measuring nodules very small.

The evaluation by overlapping circles is a time-consuming method, due to the large number of nodules to be measured, which may require approximately 8 h for the analysis of each micrograph. With the *Image J program*, the evaluation of each micrograph takes less than 15 min. Thus, the program proves to be an excellent option for analyzing many images, as in the case of mapping the microstructure of a FFN ingot in the present work.

EVALUATION OF THE QUANTITY AND SIZE OF GRAPHITE NODULES IN DIFFERENT REGIONS OF THE SAMPLE

The quantitative evaluation was carried out with three different ways of observing microstructure variation: (i) by vertical variation (column 10); (ii) by the horizontal variation (lines 10 and 40); and (iii) sample as a whole (see Figure 1-c). The data obtained by quantifying the number of nodules are presented in Figures 7 and 8 and Tables 3 to 7 with different diameter ranges: Range I – 10 to 40 μm , Range II – 41 to 70 μm , Range III - 71 to 100 μm and Range IV – 101 to 130 μm .

Through the analysis of Figure 7, it is observed that the nodules vary in quantity and size according to the vertical direction on column 10 of the sample. It is observed that there is a decrease in the number of small nodules (Range I – 10 to 40 μm) in the central region of the sample, when compared to regions close to the extremity. Large nodules (Range IV – 101 to 130 μm) are only present

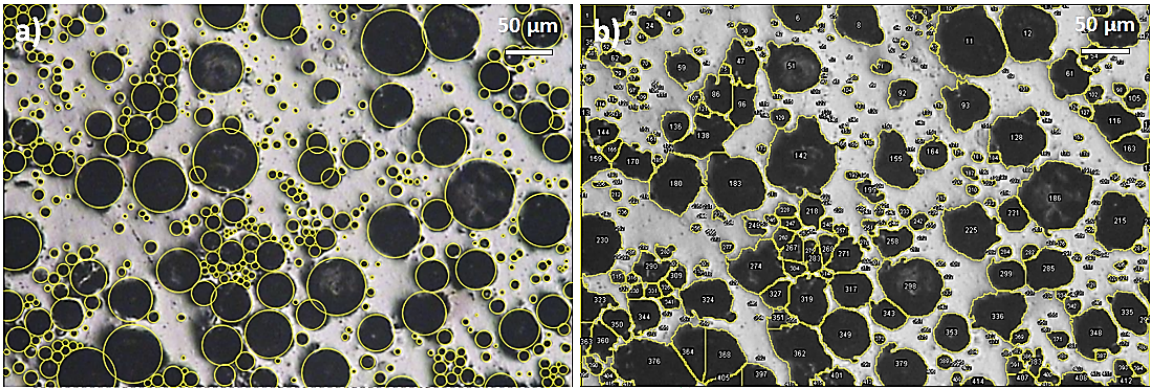


Figure 5: Illustration of the measurement methods through overlapping circles (a) and using the image *J program* (b) for the region (15,5).

Method used	Average size (μm)	Number of nodules per mm^2	Volume fraction (%)
Circular	14.5	958	38.3
Image <i>J Program</i>	21.6	1231	46.4

Table 2: Results of nodule size assessment for the region (15,5).

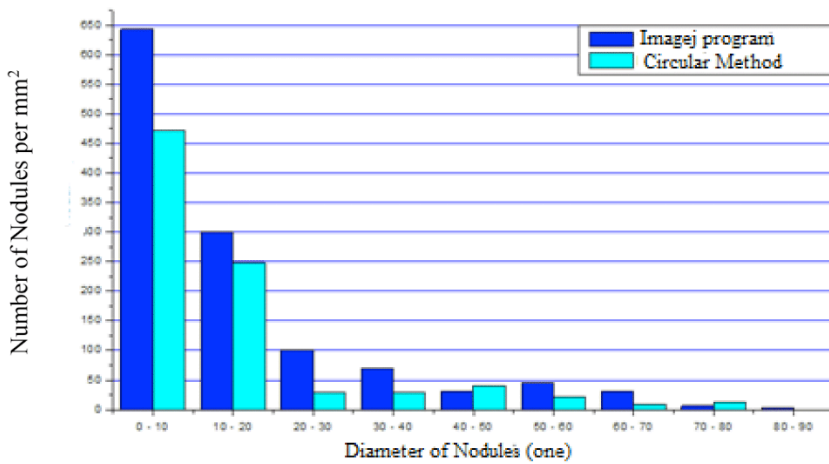


Figure 6: Comparison between the results of nodule measurements using the circle method and the Image *J program* in the region (15,5).

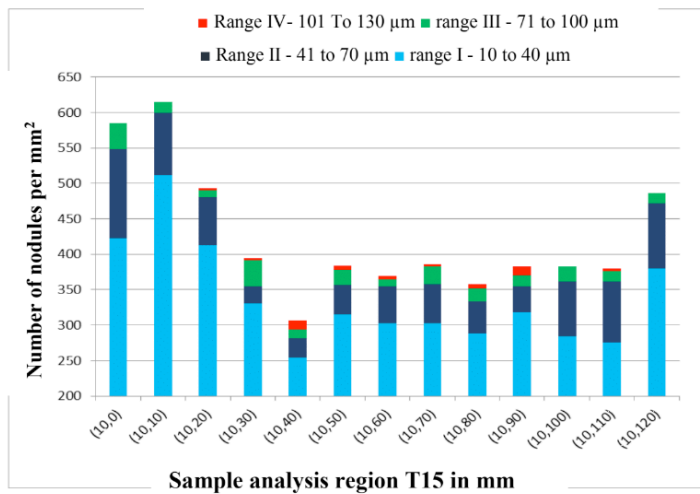


Figure 7: Histogram of the amount of graphite nodules per mm² according to their respective diameters and position in column 10 of sample T15.

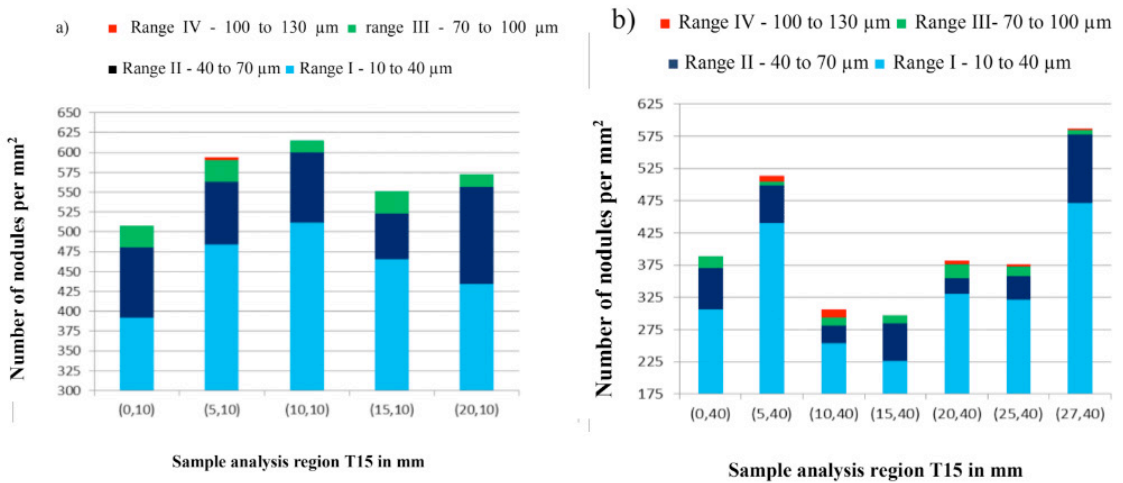


Figure 8: Histogram of the amount of graphite nodules per mm² according to their respective diameters and position in line 10 (a) and line 40 (b) of sample T15

Ingot region in mm	Number of nodules per mm ²	Average Diameter (μm)	Volume fraction (%)
(0,10)	2039	17.2	48.6
(5,10)	1283	22.4	45.1
(10,10)	1457	20.4	48.4
(15,10)	1381	20.9	48.1
(20,10)	970	20.3	51.4

Table 3: Results of quantitative analysis of line 10 of sample T15.

Ingot region in mm	Number of nodules per mm ²	Average Diameter (μm)	Volume fraction (%)
(0.40)	1166	19.0	34.3
(5.40)	1160	22.7	36.3
(10.40)	667	24.6	33.0
(15.40)	722	20.7	25.0
(20.40)	937	21.6	35.0
(25.40)	958	20.4	32.3
(27.40)	1200	22.3	48.2

Table 4: Results gives analyze quantitative of line 40 of the T15 sample.

Line (mm)	Column (mm)							
	0	5	10	15	20	25	30	35
0	1310	1482	1111	1044	1185			
10	2103	1283	1482	1402	995			
20	1194	1264	1160	670	961	1068		
30	1154	1074	777	716	894	1059	1362	
40	1206	897	692	744	961	986	1231	
50	1258	909	1194	1016	842	1635	1111	
60	1209	1166	934	1013	1163	1108	2097	
70	903	937	1024	1149	1096	774	1411	
80	1010	1231	1059	823	814	1267	1837	
90	1022	1007	787	817	970	860	1583	2155
100	1726	1148	1136	1105	1007	826	1381	1341
110	1426	1601	1546	1203	1185	1123	1374	1696
120	1788	1647	1628	1387	1549	1583	1264	2188

Table 5: Number of nodules per mm² in the entire T15 sample mapping. Darker regions are regions with a higher concentration of nodules.

in regions close to the center of the sample, with a higher incidence at points (10.40), (10.50), (10.60), (10.70), (10.80) and (10.90).

The total amount of nodules found in the sample analysis varies according to the region of the ingot. According to Rebrasa *et al* (2002), the amount of graphite nodules can vary according to several factors, mainly associated with solidification. Higher heat transfer rates increase the number of nodules. FFN ingots with a thickness of less than 3 mm can produce more than 2000 nodules per mm².

The results of the quantitative evaluation of the variation in size and number of nodules, according to horizontal lines 10 and 40 (Figure 1-c), are shown in the histograms in Figure 8 and in Tables 3 and 4.

From the histogram of line 10, Figure 8 (a), it can be seen that small nodules (Band I) are the majority, with values in the order of 450 nodules per mm². There is also a significant presence of intermediate nodules (Ranges II and III). However, large nodules (Band IV) were only recorded at point (5,10). This result is expected because, as observed in previous analyses, regions closer to the surface of the ingot, such as line 10, tend to have smaller nodules. On the other hand, on the histogram of line 40, Figure 8 (b), which is closer to the center of the ingot, large nodules (Bands IV) were observed at several points ((5,40), (10,40), (20,40) and (25,40)). In addition, in line 40, the variation in the number of nodules per region can be seen with greater intensity than in line 10. This is due to the fact that in line 40 the sample/ingot is thicker and, consequently, has a more pronounced cooling velocity gradient.

According to Tables 3 and 4, line 10 presented a total amount of 1426±763 nodules per mm², reaching a mean diameter of 20.23±3.74 μm. Line 40, on the other hand, presented a total number of nodules of 973±425 per mm², with a mean diameter

of 21.63±3.56 μm. This way, line 10, which is closer to the upper end of the sample/ingot, has a higher number of nodules per area than that shown by line 40, which is more in the center. Line 40 has an average nodule diameter slightly larger than line 10, greatly influenced by the large number of small nodules.

Table 5 illustrates the amount of graphite nodules per mm² at all points evaluated in the T15 sample mapping. The darker the cell in the table, the greater the concentration of graphite nodules. Thus, as observed in previous analyses, the lowest concentrations of nodules are located close to the center of the ingot (lighter cells in Table 5). While in regions close to the ends of the sample the concentration of nodules is higher (darker cells in Table 5). Thus showing a concentration gradient of graphite nodules. Regions of the ingot that cool more quickly, closer to the surface, have a greater number of nodules per area than regions that cool more slowly, such as in the center of the ingot.

The variation in the size and quantity of graphite nodules by region of the sample, observed during the qualitative and quantitative evaluation, may be associated with the difference in cooling speed. The cooling is not homogeneous, as regions at the end of the ingot, in contact with the mold, cool more quickly than the central regions. The concentration of graphite nodules in the center of the ingot is lower, which may be associated with the union or coalescing of the nodules. As the heat is retained in the center of the ingot for a longer time, the material remains in a liquid state for a longer time, which facilitates the coalescing of the nodules, whose driving force is the decrease in free energy, due to the decrease in the contact area between coexisting phases. In addition, under high temperature conditions, the C diffusion process is more intense, which facilitates the growth of nodules.

At the ends of the ingot, with a higher cooling speed, solidification quickly occurs, which restricts the movement and coalescing of the nodules and hinders the diffusion of C, due to lower temperatures. Still at the ends, with more intense heat removal, the supercooling effect is greater, promoting thermodynamic advantage for nucleating a greater amount of graphite nodules, with a smaller critical size and increasing the interface area between the present phases.

SUMMARY AND CONCLUSIONS

Based on the results obtained from the systematic study of changes in the morphology of a nodular cast iron ingot cast in a sand mold, it was possible to draw the following conclusions:

- The macrograph of the cross-section of the ingot revealed the presence of pores and voids in its central region. Coming from the foundry process, where during solidification gases are emitted and retained in the metallic matrix.
- According to the qualitative and quantitative analysis, the size and density of graphite nodules in nodular cast iron changes according to the region of the ingot. Regions closer to the end or surface of the ingot have a higher concentration of graphite nodules than regions located in the center, on the other hand, in the center of the ingot, the graphite nodules are larger than in regions close to the ends. This can be explained by the cooling velocity gradient, which in regions closer to the surface of the ingot is more intense than in the center.
- The variation in the speed at which cooling occurs is a determining factor for the change in the microstructure of the nodular cast iron ingot.
- Through the quantitative evaluation

and concordance of the results obtained in the measurement and quantification of graphite nodules, the ImageJ software proved to be effective for the evaluation of nodular cast iron. Mainly when compared to traditional techniques, such as overlapping circles, due to its speed of application, which allows it to be used in a large number of micrographs.

ACKNOWLEDGMENTS

The authors thank the technical and teaching staff of LAMAV-CCT-UENF, and especially Prof. doctor Fabio Duncan de Souza from IFF – Campus Campos Centro, for all his help in adapting the *Image J program* for this work.

REFERENCES

BALDAM, R.L., VIERA, E.A. **Foundry, Processes and Technologies**. Ed. Erica, 1ª edition, 384 p, 2013.

CHIAVERINI, V. **Steel and cast iron**, 7ª edition, São Paulo: Associação Brasileira de Metalurgia e Materiais – ABM, p. 494-581, 2012. ISBN: 978-85-7737-041-2

E. FRAŠ, E.; GÓRNY, M. **Inoculation Effects of Cast Iron**. *Archives of Foundry Engineering*, v.12, Is. 4, p.39-49, 2012. ISSN: 1897-3310

GUESSER, W. L. **Mechanical properties of cast iron**, 2ª edition, São Paulo: Blucher, 2019. ISBN: 9788521205012

LACAZE, J.; DAWSON, S.; HAZOTTE, A. **Cast Iron: A Historical and Green Material Worthy of Continuous Research**. *International Journal of Technology*, 12: pp.1123-1138, 2021.

NORMA ISO 945-1/2019. **Microstructure of cast irons – Graphite classifications by visual analysis**, 2019.

REBASA, N.; DOMMARCO, R.; SIKORA, J. **Wear resistance of high nodule count ductile iron**. *WEAR*, n. 253, p. 855-861, Jun. 2002.

SANTOS, A. B. de S.; BRANCO, C. H. C. **Metallurgy of gray and nodular cast iron**. São Paulo. IPT, 206p, 1989.

STEFANESCU, D. M. **Solidification and modeling of cast iron-A short history of the defining moments**. *Materials Science and Engineering*. A 413-414, p. 322-333, 2005.

VIDAL D. F. **Structural changes and mechanical properties of nodular cast iron with variable Mg content as a function of time and pouring temperature**, in Portuguese: “Alterações estruturais e propriedades mecânicas de ferros fundidos nodulares com teor de mg variável, em função do tempo e da temperatura de vazamento”. Doctoral thesis. Universidade Estadual do Norte Fluminense Darcy Ribeiro – UENF, 2017.

VIDAL, D. F. **Analysis of the structure and mechanical properties of a nodular cast iron in the foundry process produced by the bell immersion technique**, in Portuguese: “Análise de estrutura e propriedades mecânicas de um ferro fundido nodular em processo de fundição produzido pela técnica de imersão de sino”. Master thesis. Universidade Estadual do Norte Fluminense Darcy Ribeiro – UENF, 2013.